Rare Met. (2020) 39(6):636–650
https://doi.org/10.1007/s12598-020-01433-1

RARE METALS
www.editorialmanager.com/rmet

Microalloying Al alloys with Sc: a review

Jin-Yu Zhang, Yi-Han Gao, Chong Yang, Peng Zhang, Jie Kuang, Gang Liu*, Jun Sun

Received: 18 October 2019 / Revised: 20 February 2020 / Accepted: 24 April 2020 / Published online: 26 May 2020

Abstract As a kind of important light alloys, the Al alloys exhibit mechanical properties that are closely related to the microstructures. Changing the main alloying elements and adjusting heat treatments are usually approaches to tune the microstructure and hence artificially control the mechanical properties. However, the windows for the two approaches have become quite narrow, after extensive studies in the last half of century. Microalloying has become the most promising strategy to further modify the microstructure and improve the mechanical properties of Al alloys, among which the element of scandium (Sc) is especially powerful. In this paper, the recent progresses in Al alloys microalloyed with Sc are briefly reviewed, focusing on the microstructural characterization, strengthening response, and underlying mechanisms. The possible key research points are also proposed for the further development of Al alloys microalloyed with Sc and other rare earth elements.

Keywords Al alloys; Microalloying effect; Scandium; Mechanical properties

1 Introduction

The aluminum (Al) alloys, with a low density and high strength, are the primary materials of choice for industrial applications such as in aircraft, where specific strength (i.e., strength-to-weight ratio) is a major design consideration [1–3]. The high strength of heat-treatable Al alloys is mainly associated with the precipitation of excess alloying elements from supersaturated solid solution to form nano-sized precipitates that serve as effective obstacles to moving dislocations. On the one hand, the size, volume fraction, interparticle spacing, and characteristics of the precipitates will significantly affect the strengthening response [2, 4, 5]. On the other hand, the precipitations are closely dependent on the composition, processing technology, and heat treatments [6, 7]. The composition–processing–microstructure–property correlations are well manifested in the heat-treatable Al alloys. In particular, aging treatment is a commonly used approach to tune the microstructural features at nanometer length scale, where the nucleation and growth kinetics of precipitates could be artificially controlled by simply adjusting the aging temperature and aging time. Quantitatively, dynamic aging-hardening models have been proposed to describe the variation of precipitate parameters (size, volume fraction, and interparticle spacing) with aging treatment (based on precipitation thermodynamic and kinetic theories) and correspondingly the yield strength/hardness evolution (based on precipitate-dislocation interaction theories) [4–9]. This makes the precipitation hardening predictive for heat-treatable Al alloys, which promotes the Al alloys to achieve progressively increased level of performance.

Besides the optimization of aging technologies, microalloying is another effective approach to regulate the precipitation and concomitantly enhance the mechanical properties. A typical example of the microalloying effect is well documented in the Al–Cu alloys. Small addition of Sn, Cd, or In in the Al–Cu alloys was reported to suppress low-temperature aging but enhance the age hardening at elevated temperature, by facilitating the formation of θ' at the expense of GP zones and θ'' [10, 11]. Two mechanisms

J.-Y. Zhang, Y.-H. Gao, C. Yang, P. Zhang, J. Kuang, G. Liu*, J. Sun
State Key Laboratory for Mechanical Behavior of Materials, Xi'an Jiaotong University, Xi'an 710049, China
e-mail: lgsammer@mail.xjtu.edu.cn

have been proposed for this microalloying effect. One is that the microalloying elements segregate to the precipitate/matrix interface and reduce the interfacial energy [11–13]. This mechanism was first suggested to rationalize the weak X-ray reflection detected during the early stages of aging [11] and subsequently supported by indirect experimental results from calorimetric measurements [12] and transmission electron microscopy (TEM) observations [13], respectively. The other one is that the trace elements advance heterogeneous nucleation of θ′ precipitates either directly at Sn (Cd or In)-rich particles [14], or indirectly at the dislocation loops created in the as-quenched microstructure [15]. Later on, it was evidently revealed by using atom probe field ion microscopy [16] that the heterogeneous nucleation mechanism should be predominant in controlling the microstructural evolution in Sn (Cd or In)-modified Al–Cu alloys. Similarly, the heterogeneous nucleation mechanism is also responsible for some recent findings [17, 18] that minor Si or Ge additions into the Al–Cu alloys increased hardness and produced a fast hardening rate when aged at elevated temperature, where the first formed Si–Ge precipitates provided preferential nucleation sites for the metastable θ″ and then for θ′ phases.

Rare earth (RE) elements have been generally known to impact on the microstructure and mechanical properties of Al alloys even in a small addition [19]. Although early studies were mainly focused on the advantages of removing impurities and refining grains (or dendrite structure) induced by the RE addition, the RE effect on solute–solute interactions and precipitation has been attracting more and more interest, especially with the continuous progress in microstructure characterizing techniques at the atomic length scale, such as atom probe tomography (APT) [20]. At present, the RE, in particular scandium (Sc), is widely used as microalloying elements in Al alloys to control precipitation and the underlying mechanisms have been extensively investigated [21–23]. Here in this paper, we try to summarize the recent progresses in Al alloys microalloyed with Sc. In a narrow sense, the microalloying effect in Al alloys is defined that the added minor elements interact with the main alloying elements and therefore influence the nucleation/growth of inherent precipitates, which will happen in heat-treatable Al alloys, while in a broad sense, the microalloying effect could be also referred to the cases where the microalloying elements are added into non-heat-treatable Al alloys, introducing new precipitates and making the Al alloys aging-hardenable. We will discuss a broad Sc microalloying effect here. In this paper, the first part will concentrate on the non-heat-treatable Al alloys and the second part on the heat-treatable ones. It should be especially noted that only a small part of studies will be mentioned in this paper, other studies (although equally important and excellent) have to be ignored due to the limits in the text length and mostly in the authors' knowledge.

2 Non-heat-treatable Al alloys microalloyed with Sc

2.1 Pure Al

The commercial pure Al possesses good ductility and electrical conductivity, but quite low hardness or strength. The soft characteristic restricts the more applications of pure Al in industrials. While a great number of solute atoms and/or precipitates introduced in the pure Al, although increasing the hardness like in heat-treatable Al alloys remarkably reduces the ductility and simultaneously decreases the conductivity. Formation of nanosized second-phase particles with a small volume fraction is suitable to improve the strength but remain a high level of ductility and conductivity of the pure Al [5, 24, 25]. From this viewpoint, RE elements are likely the appropriate candidates, because the solubility of RE in Al is commonly low and the possibly produced RE-contained precipitates are small in volume fraction [19]. The RE addition in pure Al usually results in the formation of Al_3X (X = RE) precipitates, changing the pure Al from non-heat-treatable to heat-treatable [19]. Since the diffusion of RE is much slow in the Al matrix, the precipitation of Al_3X particles could be precisely controlled by adopting favorite aging temperature/time to reach a dispersion distribution in ultrafine size.

Sc is a typical kind of RE elements that is widely used to microalloy the Al alloys. It has been claimed [26, 27] that the Sc is the most effective precipitation hardening element per atomic fraction added compared with the elements commonly used for precipitation hardening in Al. There have been abundant studies on the Sc addition in Al alloys [26–28], but the recent hot topic on Sc-microalloyed Al alloys was boosted by a series of work from Seidman's group [19, 29–31]. Marquis and Seidman systematically investigated the evolution in size and morphology of Al_3Sc precipitates in Al with different Sc additions ($\leq$ 0.3 wt%Sc) [29, 30]. For the first time, they determined the exact morphologies of the Al_3Sc precipitates by using high-resolution transmission electron microscope (HRTEM). It was clearly revealed that the equilibrium shape of coherent Al_3Sc precipitates had 26 facets, which were the 6 {100} (cube), 12 {110} (rhombic dodecahedron), and 8 {111} (octahedron) planes, showing a great rhombicuboctahedron (Fig. 1) [29]. Both size and morphology of the Al_3Sc precipitates were found to vary with the aging treatment and Sc content. Generally, the coarsening kinetics of Al_3Sc precipitates obeyed a $(\text{time})^{1/3}$ kinetic law of the Lifshitz–Slyozov–Wagner theory, from

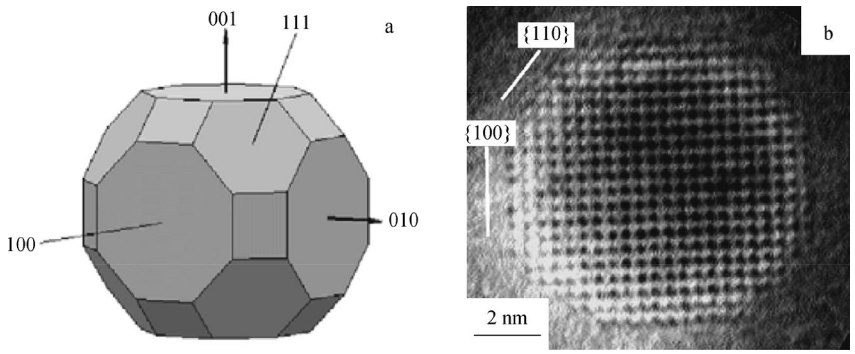

Fig. 1 **a** Wulff's construction of Al_3Sc precipitate morphology at 0 K based on first-principles calculations and **b** experimental transmission electron microscopy (TEM) image in Al–0.3wt%Sc alloy aged at 300 °C for 350 h [29]. Copyright Elsevier Ltd. All rights reserved

which the activation energy for diffusion was quantitatively determined to be $\sim (164 \pm 9)$ kJ·mol^{-1}, in good agreement with the values obtained from tracer diffusion measurements of Sc in Al and first-principles calculations [29]. It hence verified that the coarsening of Al_3Sc precipitates was diffusion-controlled. With the coarsening of the Al_3Sc precipitates, coherency would be gradually lost and the precipitate shape was reported to be spherical. Marquis and Seidman [29] claimed that the critical radius for coherency loss of Al_3Sc particles in the Al matrix was from $\sim$ 15 to $\sim$ 20 nm. Similarly, Iwamura and Miura [32] argued the critical radius from $\sim$ 15 to $\sim$ 40 nm. The conclusions drawn, respectively, by the two groups are quite close.

Strengthening effect of the Al_3Sc precipitates was subsequently studied by Marquis et al. with an aim of quantitative modeling [30]. In an elaborately designed experimental work, Al_3Sc precipitates with $L1_2$ structure were created in dilute Al–Sc alloys by varying Sc content to change the radius from $\sim$ 1.4 to $\sim$ 9.6 nm (Fig. 2a, b), which allowed to distinguish the strengthening mechanisms operating at different precipitate size regimes. The size evolution of Al_3Sc precipitate was further realized by varying aging treatment under constant Sc additions. Experimental results from room-temperature testing demonstrated that the coherent Al_3Sc precipitates significantly increased the room-temperature yield strength of aluminum by $\sim$ 6–8 times, from about 20 MPa in pure Al to 140–200 MPa in the dilute Al–Sc alloys. The precipitate radius corresponding to the peak strengthening was detected to be about 1.5 nm (Fig. 2c). The experimental results were found to agree well with the strength values predicted from the classical dispersion-strengthening theory, which indicated that the strengthening should be controlled by the precipitate shearing mechanism for smaller sizes ($< \sim$ 1.5 nm), while by the Orowan dislocation bypass mechanism for larger sizes ($> \sim$ 1.5 nm) [30].

Besides the hardening at room temperature, the Al_3Sc precipitates also make a remarkable contribution to strength at elevated temperatures. This is associated with a quite limited coarsening rate of the Al_3Sc precipitates even at elevated temperatures, due to a slow diffusion of Sc in the Al matrix [26]. The thermally stable Al_3Sc precipitates highly improve the creep resistance of the Al alloys. The Sc addition is thus exactly consistent with the criteria proposed by Knipling et al. [19] for the selection of alloying elements that are capable of producing precipitation-strengthened Al alloys with high-temperature stability and strength: these alloying elements must (1) be capable of forming a suitable strengthening phase, (2) show low solid solubility in the Al, and (3) have a low diffusion in the Al matrix.

With the aim of further improving the thermal stability of precipitates, some elements with lower diffusivity and closer location to Sc, such as Zr, were additionally added into the dilute Al–Sc alloys. In the complex addition, a strong interaction between the solutes was expected. It was evidently shown that a combined addition of Sc and Zr considerably increased the tensile strength, which was much larger than a simple sum of the single addition [31, 33–36]. The explanation from microstructural consideration was that a higher density of smaller precipitates were produced in the case of Sc + Zr co-addition, and the precipitates were also less sensitive to coarsening. By using atomic simulations as well as various advanced characterizing approaches, the underlying mechanism was revealed to be a strongly inhomogeneous structure of the precipitates [21]: due to the much faster diffusivity of Sc than Zr in the solid solution, the precipitate core was mostly Sc-rich, whereas the external shell was Zr-rich (Fig. 3). This is responsible for the observations of an enhanced nucleation rate in the Al–Zr–Sc alloys compared with the binary Al–Sc alloys, and of a much higher resistance to Ostwald ripening. This anti-coarsening effect is due to the Zr-rich shell acting as a barrier to Sc moving across the shell region [21].

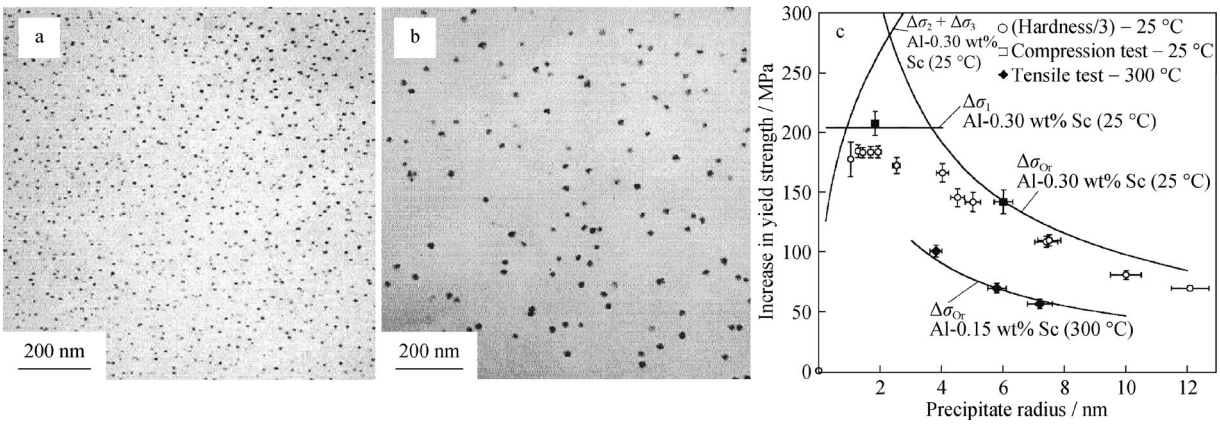

Fig. 2 **a** TEM image of Al_3Sc precipitates with an average size of ~ 1.4 nm in Al–0.3wt%Sc alloy aged at 300 °C for 72 h; **b** TEM image of Al_3Sc precipitates with an average size of ~ 9.6 nm in Al–0.1wt%Sc alloy aged at 300 °C for 72 h; **c** increase in yield stress as a function of precipitate radius for an Al–0.3wt%Sc alloy aged at different temperatures [30]. Copyright Elsevier Ltd. All rights reserved

The core–shell $Al_3(Sc, Zr)$ precipitates show more advantages besides their conspicuous strengthening response. On the one hand, the shell part enriched with Zr of slow diffusivity retards the precipitate coarsening, opening a new pathway to create thermally stable nano-sized strengthening particles and making the Al alloys possibly to serve at elevated temperatures. On the other hand, the introduction of Zr could partially replace the relatively expensive Sc element and hence reduce the cost. For a similar purpose, other transition metal elements, such as Ti or Hf, were also added into the dilute Al–Sc alloy to substitute for Sc in the $L1_2$-ordered-$Al_3(Sc,M)$ precipitates (M = transition metal element) [37, 38].

As compared to these transition metals, heavy rare earth elements, including Er, Tm, Yb, and Lu, substitute in a larger quantity within the Al_3Sc precipitates [39], which can substantially replace more of the expensive Sc. These REs also increase the lattice parameter mismatch between the $Al_3(Sc, RE)$ precipitates and the α-Al matrix, thus enhancing the elastic interactions with dislocations and improving the creep resistance of the alloys [40]. Especially, Er is the most effective and the cheapest RE [41]. Generally, Er diffuses faster than Sc in Al at aging temperature ≥ ~ 300 °C [41]. A minor Er addition into the dilute Al–Sc alloys will lead to the formation of another kind of core–shell-structured precipitates where Al_3Er rather than Al_3Sc serves as the core and $Al_3(Sc, Er)$ as the shell (Fig. 4a, b) [41]. In this case, the high-temperature creep resistance of Al–Er–Sc alloys was significantly improved in comparison with the binary Al–Sc alloys, due to a smaller lattice parameter mismatch between the precipitate shell and the Al matrix. Formation of these complex precipitates also impacts on the diffusivity of Er atoms. Karnesky et al. [41] performed careful measurements in an Al–0.06Sc–0.02 Er (at%) alloy aged at 300 °C. Their experimental results surprisingly showed that the diffusivity of Er in the ternary alloy was about three orders of magnitude smaller than that of Er in binary Al–0.045at%Er and about two orders of magnitude smaller (rather than faster) than the diffusivity of Sc in binary Al–Sc, while the diffusivity of Sc was not changed, being consistent with that in binary Al–Sc alloys. This clearly proves a significant interaction between the microalloying atoms that should be further investigated in the future.

The Al_3Sc-based core–shell complex precipitates have triggered further researches on the metallurgical physics in phase transformation of heat-treatable Al alloys. It is well known that the size distribution of particles is important for the mechanical behavior of alloys that derive their strength from a dispersion of nanoscale precipitates. In general, the particle size distributions formed by solid-state precipitation are not well controlled. Through an example of core–shell precipitates in Al–Sc-Li alloys, Radmilovic et al. [42] demonstrated an approach to form highly monodisperse particle size distributions by simple solid-state reactions. This approach involved an application of a two-step heat treatment. During the two-step heat treatment, the core was firstly formed at a higher temperature, providing a template for subsequent growth of the shell at a lower temperature (Fig. 5) [42]. Once the core was grown to a sufficient size, the shell developed in a so-called size focusing regime, where the smaller particles grew faster than the larger ones [42]. Apparently, this excellent work suggested a strategy to manipulate precipitate size distributions in similar systems through simple variations in the heat treatments.

Besides the substation of Sc atoms in Al_3Sc precipitates, the Al atoms could be also replaced by other elements. Experimental results showed $L1_2$-structured Si-containing Al_3Sc precipitates formed in an Al–0.16Sc–0.05Si (wt%) alloy aged at 300 °C [43]. Corresponding first-principles calculation indicated that the Si atoms tended to substitute Al sites in the Al_3Sc precipitates, and thus, the precipitates

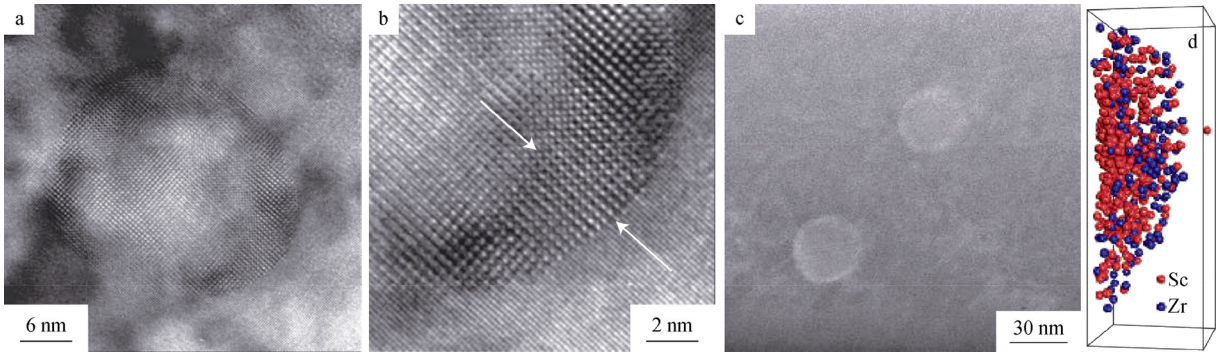

Fig. 3 Representative HRTEM images to show an $Al_3(Sc,Zr)$ precipitate with different crystal structures between core part and shell part: **a** in low magnification and **b** in high magnification; **c** a high-angle annular dark-field (HAADF) image to show core–shell structure of $Al_3(Sc,Zr)$ precipitates; **d** APT analysis of edge of an $Al_3(Sc,Zr)$ precipitate, showing a Zr enrichment at periphery (size being 5 nm × 5 nm × 18 nm) [21]. Copyright Springer. All rights reserved

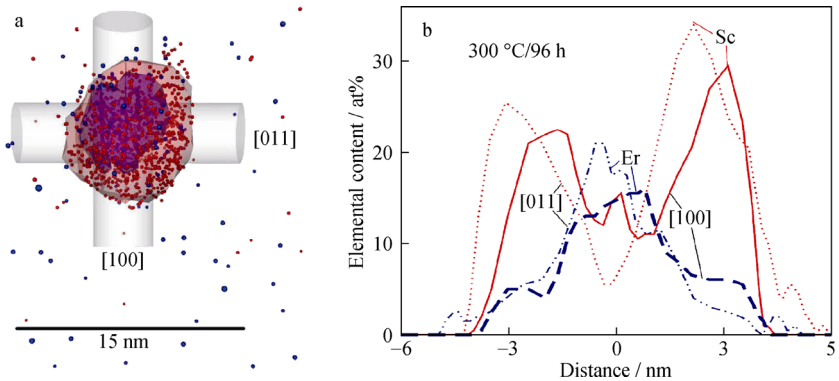

Fig. 4 **a** A representative APT image of a single $Al_3(Sc, Er)$ precipitate with concentric 5 at% isoconcentration surfaces for Sc and Er showing Er-core and Sc-shell structure; **b** concentration profile along the orthogonal cylinders in **a** for two directions, [011] and [100] showing core–shell structure quantitatively [41]. Copyright Elsevier Ltd. All rights reserved

could be represented as $(Al,Si)_3Sc$. The $(Al,Si)_3Sc$ had a dramatic precipitation-strengthening effect in the cast Al–Sc–Si alloy. However, more details on the precipitate size, distribution, and coarsening resistance were not provided in the report, and further studies are required to understand the microalloying response comprehensively.

Although Sc is the most studied RE element to microalloy pure Al [44–51], some studies were also focused on other cheaper RE elements. Typically, Nie's group mainly used Er rather than Sc to achieve a microalloying effect [52–55]. In the case of Er addition, Al_3Er precipitates were produced, just like the Al_3Sc formation under Sc addition. Nie's group firstly determined the solubilities of Er in Al at different temperatures. According to the solubility curves, they subsequently evaluated the largest volume fractions of Al_3Er to be ~ 0.18%, which was obviously less than that of Al_3Sc (~ 0.92%). However, calculations on the nucleation of trialuminides suggested that the Al_3Er showed a smaller critical radius and a larger steady state nucleation rate than the Al_3Sc. This implies a higher number density of fine precipitates could be possibly created in the Al–Er alloys. They further found in experiments that a maximum aging hardness of 400 MPa due to the precipitation of Al_3Er could be reached in an Al–0.04Er (at%) alloy aged at 350 °C [53], while in an Al–0.04Er–0.08Zr (at%) alloy, a maximum hardness of 560 MPa was recorded that was significantly greater than the Al–Er or Al–Zr binary alloys. The synergetic effect of Er and Zr on the precipitation hardening of Al–Er–Zr alloys was manifested to be a result of core–shell structure with Zr segregated in the shell of the $Al_3(Er,Zr)$ precipitates. With increasing the Zr addition, the lattice parameter of precipitates would be much closer to that of the $L1_2$-structured Al_3Zr, so the misfit between the precipitate and the Al matrix decreased and the critical size for coherency losing increased. In a recent study, the Nie's group further added minor Hf into the Al–Er–Zr alloy, and finally obtained a maximum hardness up to 662 MPa in an Al–0.045Er–0.08Zr–0.1Hf alloy aged at 350 °C [54]. The high hardness was rationalized by a sequential precipitation

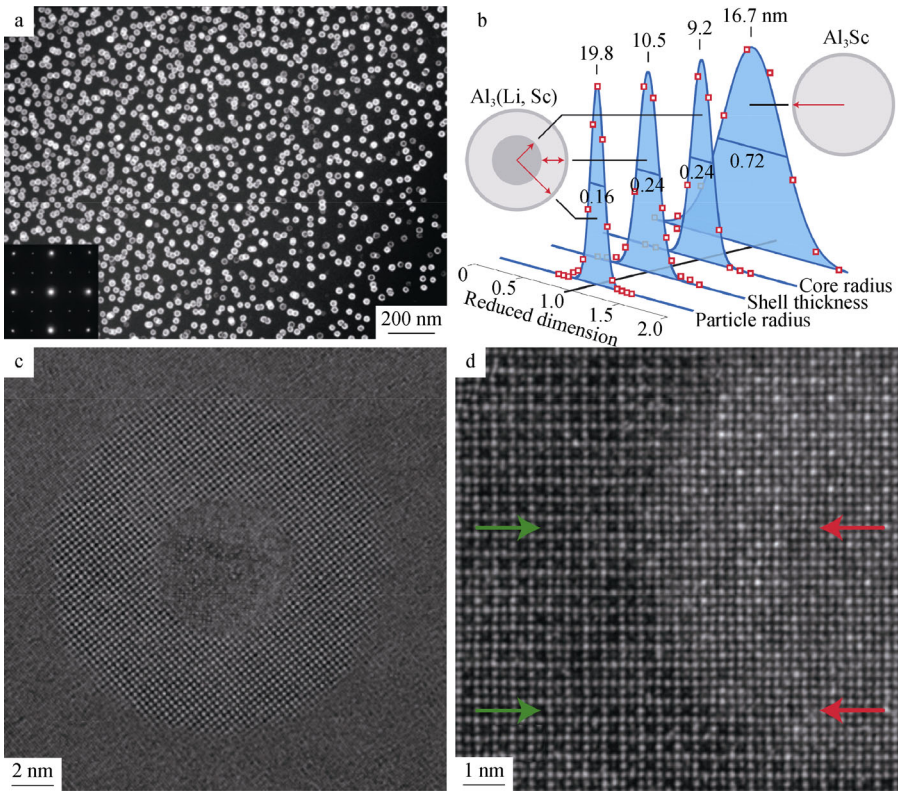

Fig. 5 **a** Dark-field micrograph of an Al–8.46Li–0.11Sc (at%) alloy, showing a remarkably uniform distribution of core–shell precipitates with $L1_2$ structure (selected area diffraction pattern inset showing strong fcc reflections and weaker $L1_2$ superlattice reflections in a square pattern typical of an <001> crystal orientation); **b** particle size distributions comparing core, shell and core–shell sizes in Al–Li–Sc alloy with much broader distribution of a typical AlSc binary alloy; **c** HRTEM image and **d** HAADF image of core–shell interface where arrows in **d** show perfect alignment of (Sc, Li) sublattice (red arrows) in core with the Li sublattice (green arrows) in shell [42]. Copyright Springer. All rights reserved

of solute elements in terms of the disparity in their intrinsic diffusivities (i.e., $D_{Er} > D_{Zr} > D_{Hf}$). Sun et al. [56] added trace Y and Zr into pure Al, and they found the grain size was refined and eutectic Al_3Y phase particles were formed within the grain interior and at the grain boundaries in the as-cast Al–Zr–Y alloys. The increase in Y additions resulted in more eutectic Al_3Y particles with larger size. The decomposition of solid solution led to a high number density of secondary $L1_2$-structured $Al_3(Zr,Y)$ precipitates within the dendritic regions during isothermal aging treatment. The recrystallization resistance of Al–Zr–Y alloys was somewhat improved by increasing the Y addition. However, excess Y addition, e.g., > 0.16%, was detrimental to the recrystallization resistance, due to the particle-simulated nucleation related to the micron-sized Al_3Y phase.

2.2 Al–Mg alloys

The Al–Mg alloys are a kind of Al alloys that are not heat-treatable. Therefore, the Sc could be also used to microalloy the Al–Mg alloys, as in the pure Al. A difference between the Al–Mg alloys and the pure Al is that Mg atoms are present in the formers, which may strongly interact with the RE atoms and highly affect the aging response. For example in an Al–2.2Mg–0.12Sc (at%) alloy aged at 300 °C [57], it was clearly revealed by APT that there were some Mg atoms segregated at the perfectly coherent Al matrix/Al_3Sc heterophase interface (Fig. 6). Ab initio calculations demonstrated that the driving force for Mg segregation was due to electronic interactions rather than elastic strain relaxation associated with highly oversized Mg atoms. The calculated value of the relative Gibbs excess of Mg with respect to Al and Sc was ~ 1.2 atoms·nm^{-2}, which was in good agreement with the experimental value. The Mg segregation lowered the free energy of {110} and {111} orientations by 10–20 mJ·m^{-2} relative to {100} orientations [58]. In addition to the interfacial Mg segregation, Mg located at the centers of Al_3Sc precipitates was also detected, which was kinetically trapped since Mg is insoluble in Al_3Sc. The diffusivity of Mg in Al_3Sc was estimated to be 2×10^{-23} m^2·s^{-1}, which was approximately seven orders of magnitude smaller than that of Mg in pure Al at 300 °C (1.62×10^{-16} m^2·s^{-1}). These will definitely reduce the growth/coarsening rate of

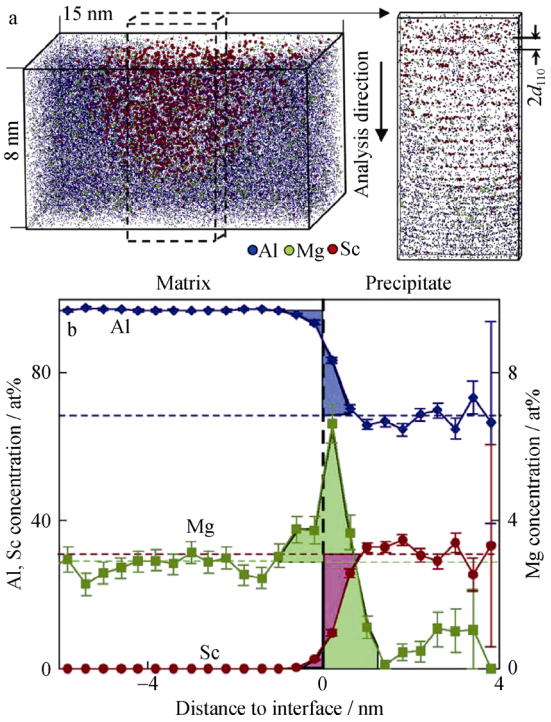

Fig. 6 **a** Three-dimensional reconstruction of an Al_3Sc precipitate in Al–2.2Mg–0.12Sc alloy after aging at 300 °C for 1040 h; **b** proximity histogram of Al_3Sc precipitate in **a**, where colored areas correspond to interfacial excesses of Al (blue), Mg (green), and Sc (red) [57]. Copyright Elsevier Ltd. All rights reserved

Al_3Sc precipitates and resultantly improve the creep resistance.

Like in the pure Al, the Sc and Zr co-addition was also applied in the Al–Mn alloys [59–62]. In an Al–Mg–Sc–Zr alloy produced through conventional rolling and annealing process, a high thermal stability and a high yield strength of about 320 MPa were achieved [59]. Microstructural examinations revealed that complex effects of solute Mg atoms and Al_3(Sc,Zr) precipitation promoted the formation of bimodal grain microstructure with large lattice misfit and sub-grains. The authors claimed that the high strength was related to the solid-solution strengthening of Mg, sub-grain and fine grain strengthening, and Al_3(Sc,Zr) precipitation strengthening [59]. In an Al–3.02Mg–0.2Sc–0.1Zr (wt%) alloy produced by selective laser melting, a tensile strength of about 373 MPa was obtained together with a great elongation of 32.5% [61], which was mainly related to the formation of nanosized Al_3(Sc,Zr) precipitates. In addition, the Sc and Zr co-addition will also refine the grain size and modify the dispersoids in the Al–Mg alloys. In an Al–5Mg–0.7Mn (wt%) alloy added by Sc and Zr, the formation of primary Al_3Sc and Al_3(Sc,Zr) refined the Al_6(Mn,Fe) dispersoids, increased the dispersoid number density, and made the dispersoid shape more regular [62]. The grain refinement and finely dispersed Al_6(Mn, Fe) phase improved the mechanical properties and increased the corrosion resistance.

2.3 Al–Si alloys

The microstructure of cast Al–Si alloys normally contains coarse primary Al and plate-like eutectic (Al/Si) phases [63]. Mechanical properties of the Al–Si alloys are closely dependent on the microstructure features. Generally, the smaller the microstructure features are, the higher the strength/hardness is. As to the ductile fracture, the coarse and lamellar structures are more prone to crack under the applied loading, while the finer structures are capable of delaying damage. Therefore, how to form a fine microstructure is very important for the Al–Si alloys. Recently, it has been found that some RE elements such as Ce and Sc could refine both the Al matrix and the eutectic (Si) of the Al–Si cast alloys [63, 64]. The underlying mechanism for the refinement of eutectic Si was proposed as follows [64]. On the one hand, the nucleation of (Si) was retarded by absorbing RE on the nuclei interface within the solidification process, which induced the eutectic (Si) nucleation at a larger undercooling. On the other hand, the growth of (Si) was also limited, due to two possible refining mechanisms of twin plane re-entrant edge mechanism [65] and impurity-induced twinning mechanism. In a Y-microalloyed hypoeutectic Al–7.08Si (wt%) alloy [66], for example, the cooling rate was found to be a critical influencing factor: at a low cooling rate, Y modified the eutectic (Si) by introducing additional nucleation cores during the nucleation process, while at a high cooling rate, Y modified the eutectic (Si) by promoting the twin formation during its growth process. However, the predominant mechanism is not well known at present, and more ongoing studies should be urgently required.

There has been another claim that, in the Sc-microalloyed Al–Si alloys, $AlSc_2Si_2$ phase (or V-phase) was produced that dominated the microalloying response [64]. The $AlSc_2Si_2$ phase was partially coherent with both Al matrix and the eutectic (Al) (Fig. 7). The semi-coherent interfaces made it possible for a great number of dislocations accommodated at the Al–Si–Sc alloys, which improved both the mechanical strengths/hardness and the ductility. This work demonstrated that an artificial introduction of hard phases (even in micrometer scale), once partially/fully coherent with the Al matrix, provides an alternative dimension for tailoring properties and performance of the Al alloys [64].

The Sc addition has also obvious effect on the mechanical properties of high-Si Al–Si alloys used for electronic packaging. In an Al–50%Si alloy, minor Sc addition (0.3%) was found to increase the tensile strength, flexural strength, and hardness by 16.2%, 8.9%, and 14.7%,

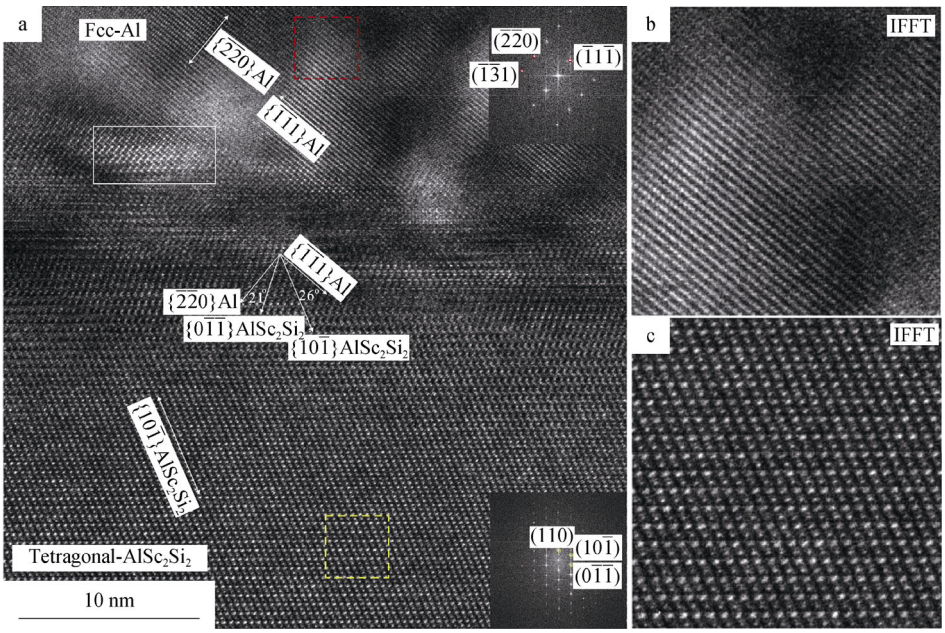

Fig. 7 **a** A representative HRTEM image of Region B marked with white dotted square to show partially coherent interface between eutectic (Al) and $AlSc_2Si_2$; inverse fast Fourier transformation of regions in **a** marked by **b** red and **c** yellow square [64]. Copyright Elsevier Ltd. All rights reserved

respectively [67]. The thermal expansion coefficient and thermal conductivity coefficient were decreased only slightly with Sc addition. Microstructural observations demonstrated that fine spherical Sc-rich particles, determined as $AlSc_2Si_2$, were produced in the Sc-microalloyed Al–Si alloy. It was then proposed that the increase in strength was mainly attributed to the $AlSc_2Si_2$ phase that strengthened the Al matrix [67]. However, the formation of incoherent $AlSc_2Si_2$ phase will definitely degraded the ductility of alloys, in comparison with the coherent Al_3Sc phase.

2.4 Other non-heat-treatable Al alloys

Ma et al. applied hot rolling, solid-solution treatment, and friction stir processing to Al–20Zn and Al–20Zn–0.5Sc (wt%) alloys to investigate the Sc effect on Al–Zn alloys [68]. They found that Sc addition refined the grains in any state and the dynamic precipitation was promoted by Al_3Sc phase. A combination of high strength and good ductility was achieved with Sc addition. In particular, the fine grains and high density of Al_3Sc particles with grain boundary pinning effect led to increased high-temperature internal friction value and excellent damping stability.

In an Al–Mn alloy produced by selective laser melting process, Sc addition was utilized to create a high strength Al alloy with a yield strength of up to 560 MPa and a ductility of about 18% after a simple industrially desirable post-heat treatment at 300 °C [69]. The high strength was mainly ascribed to a high solid-solution strengthening effect from Mn and simultaneously precipitation strengthening from a high density of nanosized Al_3Sc precipitates. This advanced Al alloy, promoted by Sc, offers tremendous benefits for the fabrication of complex high-performance lightweight engineering components made by selective laser melting process.

Eutectic Al–Ni alloys are also promising for application at high temperatures, where their high strength at elevated temperature was derived from Al_3Ni microfibers formed during solidification [70–73]. Dunand et al. investigated the possible Sc microalloying effect in Al–6%Ni (wt%) by comparing binary Al–6%Ni and Al–Sc alloys [74]. They found no noticeable Sc effect on the Al_3Ni microfiber formation, composition, and hardening response. Similarly, there was no apparent effect of Ni on the hardening of the Al_3Sc precipitates, although 0.14at%–0.17at%Ni was detected in the Al_3Sc precipitates [74]. This means that the Ni and Sc did not interact during the precipitation, and the contributions of Al_3Ni and Al_3Sc phases to room-temperature strength were simply added linearly. When crept at 300 °C, all the alloys showed a creep threshold stress, which hinted that both the microsized Al_3Ni and nanosized Al_3Sc impeded dislocation motion [74].

3 Heat-treatable Al alloys microalloyed with Sc

As reviewed above, the usage of Sc to microalloy pure aluminum or non-heat-treatable Al alloys (e.g., Al–Mg and Al–Si alloys) has been extensively investigated, mainly due

to two advantages. The first one is to strengthen these non-heat-treatable Al alloys by forming Al_3Sc precipitates, making them heat-treatable and creep-resistant. The second is to use Al_3Sc precipitates as model particles for studying basic principles in physical metallurgy, including coarsening behaviors and interaction with dislocations. On the other hand, there have been also increasing studies on the Sc (and other RE) microalloying in heat-treatable Al alloys [75–78]. However, it is relatively hard for Sc addition to further strengthen the heat-treatable Al alloys by additionally forming Al_3Sc precipitates. The Al_3Sc precipitates difficultly coexist with other strengthening precipitates, because the aging temperature regime for Al_3Sc precipitation is between the temperature regimes for aging treatment and solution treatment of common heat-treatable Al alloys [26]. Therefore, the Sc microalloying in heat-treatable Al alloys is mainly to affect the nucleation/growth/coarsening of the intrinsically formed precipitates. Note that carefully designed heat treatments, such as two-step aging treatment and aging with temperature gradually increased [79, 80], could lead to the coexistence of Al_3X (X = RE or Zr) and traditional precipitates. However, the controlling window for aging treatment is quite narrow and this is not the topic in present paper.

3.1 Al–Cu-based alloys

Al–Cu-based alloys are a kind of well-studied precipitation-strengthening system because they form the basis for a wide range of commercial age-hardening Al alloys. Plate- or disk-like θ′-Al_2Cu is the most observed strengthening precipitate in the Al–Cu-based alloys, with coherent interfaces being their broad flat faces and semi-coherent interface at their periphery. Segregations of Si and Mg atoms at the θ′/matrix interfaces have been visibly revealed in the Al–Cu alloys with minor Si and Mg additions [58, 81], by using the APT examinations. The solute atom segregation will change the interfacial conditions (e.g., interface structure, chemistry composition, and energies) and cause a series of evolutions in both precipitation behaviors and strengthening responses, including precipitate nucleation and concomitantly number density and driving force for precipitate coarsening [81]. Solute segregation at the precipitate/matrix interfaces is an important microalloying method to tailor the precipitation and improve the hardening response.

Sc is a RE element that has been experimentally found [82, 83] to segregate at the θ′/matrix interfaces in the Al–Cu alloys (Fig. 8). Chen et al. [82] demonstrated that, in an Al–2.5Cu–0.3 Sc alloy (wt%), the microalloying Sc atoms were prone to segregate at the θ′/matrix interfaces, which promoted the θ′ precipitation and hence enhanced the strengthening response. For comparison, the Al–Cu–Sc alloy was aged at three different temperatures, i.e., 200, 250, and 300 °C, for the same time, respectively. It was found that the most interfacial Sc segregation was created in the 250 °C-aged alloy, where the interfacial Sc concentration was about 10 times greater than that in the matrix. As a result, a reduction of ∼ 25% in interfacial energy was achieved. Based on the experimental results of strength measurements and APT analyses, the authors proposed a scaling relationship between the interfacial energy and precipitation-strengthening increment [82]. This scaling relationship could semi-quantitatively rationalize the most notable strengthening effect observed in the 250 °C-aged alloy, which was about 2.5 times that of the Sc-free Al–Cu alloy and about 1.5 times that of the counterparts aged at 200 or 300 °C. Ductile fracture of the alloy was further discussed with respect to the interfacial Sc segregation. Especially in the 250 °C-aged Al–Cu–Sc alloy, a quick drop in ductility was experimentally revealed when the precipitate radius was greater than about 200 nm. This drop indicated a possible transition in fracture mechanisms. Using in situ TEM tensile testing, the authors argued that the underlying fracture mechanism for reduced ductility was the interfacial decohesion induced at the θ′ precipitates ahead of crack tip, which favorably aided the crack propagation [82].

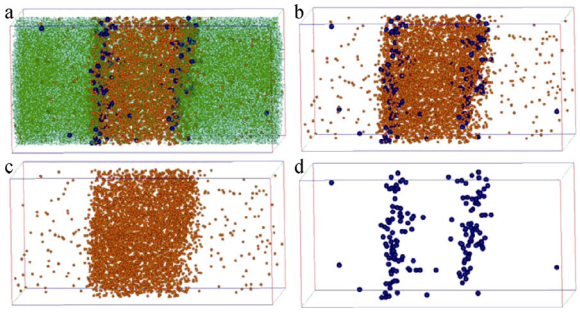

Fig. 8 **a** Representative three-dimensional atom probe (3DAP) maps to show distribution of Al, Cu, and Sc atoms across θ′/matrix interface in Al–Cu–Sc sample aged at 250 °C for 3 h (green = Al atoms, orange = Cu atoms, blue = Sc atoms, dimensions of 20 nm × 20 nm × 40 nm); **b** Cu and Sc atoms co-presented, **c** only Cu atoms presented and **d** only Sc atoms presented (Sc segregation at θ′/matrix interfaces is evident) [82]. Copyright Elsevier Ltd. All rights reserved

As a kind of heat-treatable Al alloys, the Al–Cu-based alloys are required to undergo solid-solution treatment before aging. Although the aging temperature (∼ 190 °C) of θ′ precipitation is much lower than that of the Al_3Sc precipitation, the temperature of solid-solution treatment is high enough to precipitate Al_3Sc. This means that there should be some Al_3Sc particles created during the solid-solution treatment of the Al–Cu–Sc alloys. The Al_3Sc particles formed during high-temperature treatments, i.e., homogenization and solid-solution treatments, generally have a relatively large size (e.g., several tens nanometers in

size) and are referred as "Al_3Sc dispersoids," which are different from the fine "Al_3Sc precipitates" (with a size below a few tens nanometers) formed during low-temperature aging treatment. The well-known contribution of Al_3Sc dispersoids is to stabilize the grain/sub-grain structure of Al alloys through Zener-drag action and hence enhance recrystallization resistance [26, 28]. The strengthening of Al_3Sc dispersoids is normally smaller than that of the Al_3Sc precipitates, due to a much larger size than the later ones. In the case of Al–Cu–Sc alloys with a constant Sc addition, the formation of Al_3Sc dispersoids will consume Sc atoms and hence leave less Sc atoms available for interfacial segregation in subsequent aging treatment. The Sc partitioning between Al_3Sc dispersoids and Sc segregation at the θ′/matrix interfaces should be carefully balanced to reach an optimized microalloying effect.

Yang et al. [83] systematically studied the microstructural evolution and strengthening response of Al–*x*Cu alloys (x = 1.0 wt%, 1.5 wt%, and 2.5 wt%) with 0.3wt%Sc addition. They found a dual solute alloying/microalloying effect on the microstructural evolution. On the one hand, a Cu alloying effect was evident that affected the nucleation and coarsening of Al_3Sc dispersoids. With increase in the Cu content, a decrease was detected in both the Al_3Sc dispersoid size and the volume fraction in the solid-solution condition. On the other hand, the precipitation of θ′-Al_2Cu strengthening particles during aging treatment displayed a notable Sc microalloying effect, because the precipitation was promoted by Sc segregation at the θ′/matrix interfaces. Comparisons showed that the strongest interfacial Sc segregation was generated in the Al–2.5Cu–Sc alloy, where the θ′ precipitation was most promoted. A Sc partitioning between the Al_3Sc dispersoids and interfacial Sc segregation, which could be tuned by Cu content, played an important role in strengthening response and deformation behavior. The room-temperature yield strength of the Al–2.5Cu–Sc alloy was approximately 1.8 times that of the Al–1.5Cu–Sc and Al–1.0Cu–Sc alloys [83].

To predict the solute segregation at the θ′/matrix interfaces in Al–Cu-based alloys, Shin et al. [84] constructed a large theoretical database of solute segregation energies at the coherent and semi-coherent interfaces. They analyzed the relationship between the solute segregation energies and atomistic descriptors [84]. It was generally shown that the large solutes had a strong tendency to segregate at both the coherent and semi-coherent interfaces [84]. Besides, solubility- and mixing-related factors were highly considered in the analysis. A main conclusion was drawn that the elements predicted to have a large solubility within θ′ as a result of ideal mixing behavior probably displaying favorable segregation to the interfaces. From these predictions, another RE element of Y, besides Sc, should be also thermally stable to segregate at the θ′/matrix interfaces and may produce a significant microalloying effect.

Co-addition of Sc and Zr into the Al–Cu alloy has been also investigated. In an Al–4Cu–0.1Sc–0.14Zr (wt%) alloy, Dorin et al. [85] observed that $L1_2$-type core–shell $Al_3(Sc,Zr)$ dispersoids were firstly produced during high-temperature homogenization. These dispersoids played a significant role in the nucleation and growth of θ′ during following aging treatment, since the dispersoids served as preferential nucleation sites for the precipitates (Fig. 9). The dispersoid-promoted precipitation resulted in a refined size distribution for θ′ precipitates, showing a remarkable microalloying effect [85].

It should be especially mentioned that RE elements of La and Ce have been also used [86] to microalloy the Al–Cu alloys. The creep resistance of Al–Cu–La alloys was almost 3–5 times higher than that of the La-free counterpart. It was claimed that the underlying mechanism of the La modification was mainly the formation of $Al_{11}La_3$ phases [86]. These phases were thermally stable and located at the grain boundaries and ligaments between the dendrites (Fig. 10), which inhibited the grain boundary migration and dislocation movement during creeping. Nevertheless, the presence of micron-sized $Al_{11}La_3$ phases

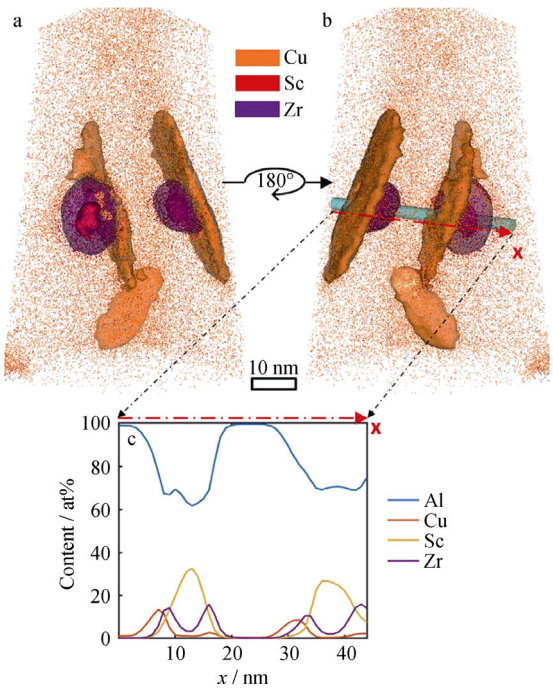

Fig. 9 **a**, **b** Representative APT images and **c** corresponding composition evolution across plate-like precipitates and dispersoids to show core–shell structure in $Al_3(Sc,Zr)$ dispersoids and θ′ particles precipitated preferentially on $Al_3(Sc,Zr)$ dispersoids [85]. Copyright Elsevier Ltd. All rights reserved

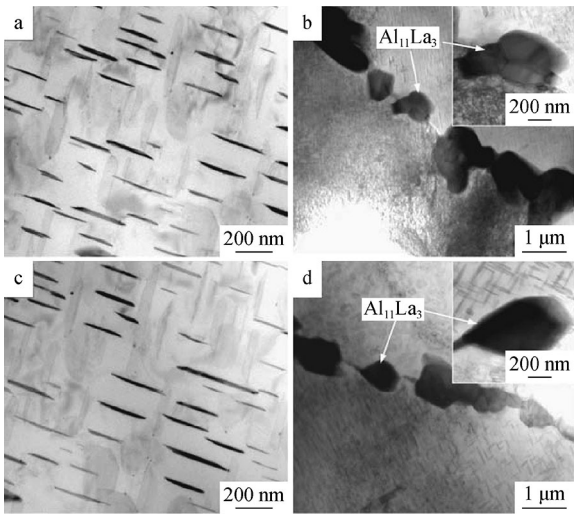

Fig. 10 Representative TEM images of **a** La-free Al–Cu alloy and **b** La-added Al–Cu alloy before creep testing, and their corresponding samples **c** La-free and **d** La-added after crept at 220 °C and a stress of 90 MPa [86]. Copyright Elsevier Ltd. All rights reserved

will dramatically reduce the ductility and fracture toughness of the Al–Cu alloys. This means that it is extremely difficult to balance the room-temperature mechanical properties and the high-temperature creep resistance in the La-modified Al–Cu alloys. In a Ce-microalloyed Al–5.8Cu–0.3Mn–0.2 Mg–0.2Zr (wt%) alloy [87], it experimentally revealed that a 0.2 wt% Ce addition promoted the precipitation of denser and finer θ′ phase, which improved the tensile strength at both room and elevated temperatures. High-melting-point Al_8Cu_4Ce phase particles were found in the alloys with Ce additions up to 0.4 wt%, which contributed to the mechanical properties at elevated temperature. Another investigation reported that an addition of Ce up to 0.45 wt% into an Al–Cu–Mg–Ag alloy induced the precipitation of finer and denser Ω and θ′ phases when compared to the Ce-free case [88]. These enhanced precipitations improved the tensile strength at both room temperature and high temperature. Besides, the addition of Ce up to 0.45 wt% also improved thermal stability of the Ω phase. These factors may promote the service temperature of the conventional Al–Cu–Mg–Ag-based alloys.

Sc addition is not always helpful for the precipitation and mechanical properties of the Al–Cu-based alloys. In an Al–Cu–Mg–Ag alloy with 0.32wt%Sc addition [89], the yield strength of alloy was found to be degraded in comparison with the Sc-free counterpart. This Sc negative effect was directly associated with the formation of Al_8Cu_4Sc intermetallics, which consumed some Cu solutes and hence limited the Cu atoms available for Ω precipitation, resulting in a slower Ω nucleation and lower precipitate number density. The Sc-promoted rapid growth of S precipitates was also found during extended aging. In addition, no apparent refinement in grain size was observed. In this case, it is evident that Sc addition is unfavorable.

3.2 Al–Mg–Si-based alloys

As a kind of important structural materials, the age-treatable Al–Mg–Si-based alloys (known as 6xxx series Al alloys) have been widely used in many fields, such as in automotive and aviation industries. A typical precipitation sequence of the Al–Mg–Si alloys follows the below order: supersaturated solid solution → early precipitation stages (GP zones) → β″ phase → β′ phase → β phase (Mg_2Si) [9]. However, the precipitation in the Al–Mg–Si alloys is quite complicated, because it is highly sensitive to the composition, heat treatments, and other factors. It has been claimed [90, 91] that the Mg/Si ratio had remarkable influence on the precipitations. Since the Mg/Si mass ratio is about 1.73 in Mg_2Si, the Mg and Si will be fully used to produce Mg_2Si particles, once the nominal Mg/Si ratio equals 1.73. Either Mg or Si in excess addition will impact on the precipitation and therefore on the mechanical properties. Previous reports showed that an increase in Si content usually resulted in more formable alloys with a higher strength [90]. The main reason was that excess Si promoted the uniform precipitation of fine β″ precipitates [90]. On the contrary, addition of excess Mg usually led to a low strength. When a minor Sc is added in the Al–Mg–Si alloys, the β″ precipitation will be further changed. It is well known that the diffusion coefficient of Si in Al matrix is much greater than that of Mg and also several orders of magnitude greater than that of Sc [92]. In the Sc-microalloyed Al–Mg–Si alloys, the formation of Si–Sc pairs is thermodynamically favored, due to a high negative enthalpy between Si and Sc atoms (~ -207 kJ·mol^{-1} [92]). This means that the originally fast Si atom diffusion would be slowed down by Sc capturing, which would significantly restrict the precipitate growth. In contrast, Mg atom diffusion is slightly affected by Sc addition, because of a weak Mg–Sc binding (with an enthalpy of only ~ -13 kJ·mol^{-1}). The Sc-induced decrease in Si diffusion could thus reduce the growth rate of β″ precipitates.

Formation of Al_3Sc-based dispersoids and their contribution to mechanical properties were still the research focus in the Sc-microalloyed Al–Mg–Si alloys. The formation kinetics of Al_3Sc has been shown [93] to be enhanced by the presence of Si, even at Si impurity levels. Similarly in the Al–Mg–Si-based alloys, the coarsening resistance of Al_3Sc could be improved by adding trace Zr, as it forms Al_3Zr shell on the Al_3Sc core, which reduces the lattice mismatch with the Al matrix, and prevents Sc from moving across the interface. Recent work by Dorin et al.

[44] on Al–Mg–Si–Sc–Zr alloys revealed solidification microsegregations in the as-cast condition. The presence of Si also caused the formation of $(Al,Si)_3(Sc,Zr)$ dispersoids in the as-cast microstructure. However, the impact of Sc on precipitation sequence in the Al–Mg–Si-based alloys is still unknown up to now. In a recent work on precipitation sequence in an Al–1Mg–0.6Si–0.1Sc–0.2Zr (wt%) alloy [93], the samples were exposed to isochronal aging from 100 to 450 °C with a 25 °C temperature step and a 3-h holding time at each temperature. At the low aging temperatures, it was claimed from hardness evolution that the presence of solute Sc and Zr had no noticeable effect on the β″ precipitation, which, however, was not proven by microstructural evidences [93]. When aged to high temperatures, the precipitation kinetics of $Al_3(Sc,Zr)$ was soundly found to be accelerated in the presence of Mg and Si, and APT results manifested that this was due to the preferred nucleation of the $Al_3(Sc,Zr)$ dispersoids on the MgSi precipitates.

3.3 Al–Zn–Mg-based alloys

The Al–Zn–Mg-based alloys are widely used in aerospace fields. Generally, the addition of Sc into Al–Zn–Mg-based alloys can effectively improve strength, refine grains, and inhibit recrystallization. The improvements of these properties are mainly due to the formation of Al_3Sc dispersoids. It is known that the Al–Zn–Mg-based 7xxx series Al alloys are susceptible to localized corrosion such as pitting, intergranular corrosion and environmentally assisted cracking [94], especially with a high content of Zn and Mg, showing a poor resistance to corrosion [95]. Adding elements, such as Cr, Zr, and RE of Sc and Yb, could improve corrosion resistance by refining grains or inhibiting recrystallization [96, 97]. The co-addition of Sc and Zr has been proved to improve the corrosion resistance of Al–Zn–Mg–Cu alloys, due to the inhibition of recrystallization behavior [96]. The spacing of grain boundary precipitates in the Al–Zn–Mg–Cu–Sc–Zr alloy was found to be larger than that in the recrystallized Al–Zn–Mg–Cu alloy, and the discontinuity of precipitates distribution along the grain boundary was also enhanced by the introduction of Sc and Zr.

Yin's group studied the Al–5.39Zn–1.91Mg–0.34Cu (wt%) alloy doped with different amounts and ratios of Sc and Zr [98]. Their results showed that the yield strength increased by 66 MPa with 0.1wt%Sc and 0.1wt%Zr, and improved by 96 MPa with 0.25wt%Sc and 0.10wt%Zr, respectively, compared with the Sc- and Zr-free counterpart. The effect of Sc/Zr ratio on the microstructure and mechanical properties of Al–Zn–Mg–Sc–Zr alloys was systematically investigated [99]. It was demonstrated [99] that the highest tensile strength was achieved by adding 0.2Sc/0.4Zr (wt%), where the most distribution density of $Al_3(Sc, Zr)$ precipitates was obtained. However, it was clearly revealed that the small additions of Sc and Zr did not retard or suppress the formation of aging η‘ precipitates in the Al–Zn–Mg–Sc–Zr alloy. The strengthening effect from η‘ precipitates was much stronger than that from the Sc and Zr microalloying response. The strength increments caused by additions of Sc and Zr were mainly derived from refinement of primary $Al_3(Sc, Zr)$ particles, substructure strengthening, and Orowan strengthening that was associated with the secondary $Al_3(Sc, Zr)$ particles formed during homogenization treatment.

In Liu et al.'s work [100] on Al–Zn–Mg–Cu alloy microalloyed by Sc and Zr, they found solute segregation of Zn, Mg, and Cu in the core–shell-structured $Al_3(Sc,Zr)$ precipitates by using APT, aberration-corrected scanning transmission electron microscopy (STEM), and first-principles simulations. The $Al_3(Sc,Zr)$ precipitates had a core enriched by Sc while shell enriched by Zr. The Zn atoms were segregated to the Zr-rich shell and substituted mainly for the Al atoms. The Mg and Cu atoms were segregated to the Zr-rich shell during the early stages of aging, while the Mg atoms preferred to the Al matrix at longer aging time. Such segregation was demonstrated by density functional theory calculations to be energetically favored [100].

Besides the Sc and Zr co-addition, a novel Al–Zn–Mg alloy with Er and Zr additions has been developed by Nie' group [101, 102]. The new type Al–Zn–Mg–Er–Zr alloy exhibited excellent comprehensive performance, such as strength, weldability, and recrystallization resistance, which was unsurprisingly attributed to the presence of $L1_2$-structured $Al_3(Er,Zr)$ nanoparticles.

4 Summaries and perspective

In summary, Sc is capable of playing an important role in microalloying Al alloys. In the non-heat-treatable Al alloys, a minor addition of Sc can lead to the formation of $L1_2$-type Al_3Sc precipitates, making the alloys heat-treatable. In the heat-treatable Al alloys, a trace Sc mostly promotes the dispersed precipitation of strengthening particles with refined size, by facilitating heterogeneous nucleation and reducing growth/coarsening drive force. The Sc microalloying effect in Al alloys usually results in improved strength, enhanced corrosion resistance, and increased thermal stability. Therefore, the Al alloys microalloyed with Sc will attract progressive attention and yield continuing results in both scientific and technological aspects. The following issues should be especially focused in the further studies: (1) multiple RE addition rather than single Sc addition to form complex precipitates with high growth/coarsening resistance; (2) interactions between Sc

atoms and the main alloying atoms and their impact on the precipitation with underlying mechanism at atomic length scale; (3) Sc microalloying effect on ductile fracture of Al alloys (not only on strength/hardness); (4) parameters directly characterizing the Sc microalloying effect and their relation to mechanical properties; (5) evolution of Sc microalloying effect during thermal and mechanical cycling service conditions; and (6) the Sc microalloying effect on other properties, including corrosion properties, electrical properties, thermal conductivity, etc., which are usually required besides the mechanical properties. These topics should be also applicable to other rare earth elements.

Acknowledgements This work was financially supported by the National Natural Science Foundation of China (Nos. 51621063, 51625103, 51722104, 51790482, and 51761135031) and the Program of the Ministry of Education of China for Introducing Talents of Discipline to Universities (No. BP2018008). This work is also supported by the International Joint Laboratory for Micro/Nano Manufacturing and Measurement Technologies.

References

[1] Hornbogen E, Starke EA Jr. Theory assisted design of high strength low alloy aluminum. Acta Metall Mater. 1993;41(1):1.
[2] Wen K, Xiong BQ, Fan YQ, Zhang YA, Li ZH, Li XW, Wang F, Liu HW. Transformation and dissolution of second phases during solution treatment of an Al–Zn–Mg–Cu alloy containing high zinc. Rare Met. 2018;37(5):376.
[3] Huang HL, Jia ZH, Xing Y, Wang XL, Liu Q. Microstructure of Al–Si–Mg alloy with Zr/Hf additions during solidification and solution treatment. Rare Met. 2019;38(11):1033.
[4] Liu G, Zhang GJ, Ding XD, Sun J, Chen KH. Modeling the strengthening response to aging process of heat-treatable aluminum alloys containing plate/disc- or rod/needle-shaped precipitates. Mater Sci Eng A. 2003;344:113.
[5] Liu G, Sun J, Nan CW, Chen KH. Experiment and multiscale modeling of the coupled influence of constituents and precipitates on the ductile fracture of heat-treatable aluminum alloys. Acta Mater. 2005;53(12):3459.
[6] Grong Ø, Shercliff HR. Microstructural modelling in metals processing. Prog Mater Sci. 2002;47(1):163.
[7] Deschamps A, Livet F, Bréchet Y. Influence of pre-deformation on ageing in an Al–Zn–Mg alloy—I. Microstructure evolution and mechanical properties. Acta Mater. 1998;47(1):281.
[8] Starink JM, Wang SC. A model for the yield strength of overaged Al–Zn–Mg–Cu alloys. Acta Mater. 2003;51(17):5131.
[9] Myhr OR, Grong Ø, Andersen SJ. Modelling of the age hardening behaviour of Al–Mg–Si alloys. Acta Mater. 2001;49(1):65.
[10] Hardy H. The ageing characteristics of ternary aluminium–copper alloys with cadmium indium or tin. J Inst Met. 1952;80(2):483.
[11] Silcock JM, Heal TJ, Hardy HK. The structural ageing characteristics of ternary aluminium–copper alloys with cadmium, indium, or tin. J Inst Met. 1955;84(1):23.
[12] Boyd JD, Nicholson RB. A calorimetric determination of precipitate interfacial energies in two Al–Cu alloys. Acta Metall. 1971;19(3):1101.
[13] Sankaran R, Laird C. Effect of trace additions Cd, In and Sn on the interfacial structure and kinetics of growth of θ′ plates in Al–Cu alloy. Mater Sci Eng. 1974;14(1):271.
[14] Kanno M, Suzuki H, Kanoh O. The precipitation of theta-prime phase in an Al–4%Cu–0.06%In alloy. J Jpn Inst Met. 1980;44(3):1139.
[15] Nuyten JBM. Quenched structures and precipitation in Al–Cu alloys with and without trace additions of Cd. Acta Metall. 1967;15(4):1765.
[16] Ringer SP, Hono K, Sakurai T. The effect of trace additions of Sn on precipitation in Al–Cu alloys: an atom probe field ion microscopy study. Metall Mater Trans A. 1995;26(5):2207.
[17] Mitlin D, Morris JW, Radmilovic V, Dahmen U. Precipitation and aging in Al–Si–Ge–Cu. Metall Mater Trans A. 2001;32(1):197.
[18] Mitlin D, Radmilovic V, Morris JW, Dahmen U. On the influence of Si–Ge additions on the aging response of Al–Cu. Metall Mater Trans A. 2003;34(2):735.
[19] Knipling KE, Dunand DC, Seidman DN. Criteria for developing castable, creep-resistant aluminum-based alloys—a review. Z Fuer Metallk. 2006;97(3):246.
[20] Ringer SP, Hono K. Microstructural evolution and age hardening in aluminium alloys: atom probe field-ion microscopy and transmission electron microscopy studies. Mater Charact. 2000;44(1):101.
[21] Clouet E, Lae L, Epicier T, Lefebvre W, Nastar M, Deschamps A. Complex precipitation pathways in multicomponent alloys. Nat Mater. 2006;5(2):482.
[22] Fazeli F, Poole WJ, Sinclair CW. Modeling the effect of Al_3Sc precipitates on the yield stress and work hardening of Al–Mg–Sc alloy. Acta Mater. 2008;56(7):1909.
[23] Robson JD. A new model for prediction of dispersoid precipitation in aluminium alloys containing zirconium and scandium. Acta Mater. 2004;52(6):1409.
[24] Liu G, Zhang GJ, Wang RH, Hu W, Sun J, Chen KH. Heat treatment-modulated coupling effect of multi-scale second-phase particles on the ductile fracture of aged aluminum alloys. Acta Mater. 2007;55(1):273.
[25] Hahn GT, Rosenfield AR. Metallurgical factors affecting fracture toughness of aluminum alloys. Metall Trans A. 1975;6(2):653.
[26] Røyset J, Ryum N. Scandium in aluminium alloys. Int Mater Rev. 2005;50(1):19.
[27] Drits ME, Pavlenko SG, Toropova LS, Bykov YG, Ber LB. Mechanism of the influence of scandium in increasing the strength and thermal stability of alloys of the Al–Mg system. Soviet Phys Dok. 1981;26(3):344.
[28] Jones MJ, Humphreys FJ. Interaction of recrystallization and precipitation: the effect of Al_3Sc on the recrystallization behaviour of deformed aluminium. Acta Mater. 2003;51(15):2149.
[29] Marquis EA, Seidman DN. Nanoscale structural evolution of Al_3Sc precipitates in Al(Sc) alloys. Acta Mater. 2001;49(7):1909.
[30] Seidman DN, Marquis EA, Dunand DC. Precipitation strengthening at ambient and elevated temperatures of heat-treatable Al(Sc) alloys. Acta Mater. 2002;50(18):4021.
[31] Fuller CB, Seidman DN, Dunand DC. Mechanical properties of Al(Sc, Zr) alloys at ambient and elevated temperatures. Acta Mater. 2003;51(19):4803.
[32] Iwamura S, Miura Y. Loss in coherency and coarsening behavior of Al_3Sc precipitates. Acta Mater. 2004;52(3):591.
[33] Knipling KE, Karnesky RA, Lee CP, Dunand DC, Seidman DN. Precipitation evolution in Al–0.1Sc, Al–0.1Zr and Al–0.1Sc–0.1Zr (at%) alloys during isochronal aging. Acta Mater. 2010;58(20):5184.

[34] Zhang CM, Jiang Y, Cao FH, Hu T, Wang YR, Yin DF. Formation of coherent, core-shelled nano-particles in dilute Al–Sc–Zr alloys from the first-principles. J Mater Sci Technol. 2018;35(5):930.
[35] Liu L, Jiang JT, Zhang B, Shao WZ, Zhen L. Enhancement of strength and electrical conductivity for a dilute Al–Sc–Zr alloy via heat treatments and cold drawing. J Mater Sci Technol. 2018;35(6):962.
[36] Sun SP, Li XP, Yang J, Wang HJ, Jiang Y, Yi DQ. Point defect concentrations of $L1_2$–Al_3X(Sc, Zr, Er). Rare Met. 2018;37(8):699.
[37] van Dalen ME, Seidman DN, Dunand DC. Creep- and coarsening properties of Al–0.06 at% Sc–0.06 at% Ti at 300–450 °C. Acta Mater. 2008;56(15):4369.
[38] Luca AD, Seidman DN, Dunand DC. Effects of Mo and Mn microadditions on strengthening and over-aging resistance of nanoprecipitation-strengthened Al–Zr–Sc–Er–Si alloys. Acta Mater. 2019;165:1.
[39] Harada Y, Dunand D. Microstructure of Al_3Sc with ternary rare-earth additions. Intermetallics. 2009;17(1):17.
[40] Karnesky RA, Seidman DN, Dunand DC. Creep of Al-Sc microalloys with rare-earth element additions. Mater Sci Forum. 2006;519–521:1035.
[41] Karnesky RA, Dunand DC, Seidman DN. Evolution of nanoscale precipitates in Al microalloyed with Sc and Er. Acta Mater. 2009;57(11):4022.
[42] Radmilovic V, Ophus C, Marquis EA, Rossell MD, Tolley A, Gautam A, Asta M, Dahmen U. Highly monodisperse core–-shell particles created by solid-state reactions. Nat Mater. 2011;10(3):710.
[43] Du G, Deng JW, Wang YL, Yan DS, Rong LJ. Precipitation of $(Al, Si)_3Sc$ in an Al–Sc–Si alloy. Scr Mater. 2009;61(3):532.
[44] Dorin T, Ramajayam M, Babaniaris S, Langan TJ. Micro-segregation and precipitates in as-solidified Al–Sc–Zr–(Mg)–(Si)–(Cu) alloys. Mater Charact. 2019;154:353.
[45] Wang ZP, Fang QH, Fan TW, Chen DC, Liu B, Liu F, Ma L, Tang PY. Effects of solute atoms on 9R phase stabilization in high-performance Al alloys: a first-principles study. JOM. 2019;71(6):2041.
[46] Dan CY, Chen Z, Ji G, Zhong SY, Li J, Li XR, Brisset F, Sun GA, Wang HW, Ji V. Cube orientation bands observed in largely deformed Al–Sc alloys containing shearable precipitates. Scr Mater. 2019;166:139.
[47] Chen D, Xia CJ, Liu XM, Wu Y, Wang ML. The effect of alloying elements on the structural stability, and mechanical and electronic properties of Al_3Sc: a first-principles study. Materials. 2019;12(9):1539.
[48] Lin JD, Seidman DN, Dunand DC. Improving coarsening resistance of dilute Al–Sc–Zr–Si alloys with Sr or Zn additions. Mater Sci Eng A. 2019;754:447.
[49] Sun J, Wang XQ, Guo LJ, Zhang XB, Wang HW. Synthesis of nanoscale spherical TiB_2 particles in Al matrix by regulating Sc contents. J Mater Res. 2019;34(7):1258.
[50] Beeri O, Baik SI, Bram AI, Shandalov M, Seidman DN, Dunand DC. Effect of U and Th trace additions on the precipitation strengthening of Al–0.09Sc (at%) alloy. J Mater Sci. 2019;54(5):3485.
[51] Okle P, Lin JD, Zhu TY, Dunand DC, Seidman DN. Effect of micro-additions of Ge, In or Sn on precipitation in dilute Al–Sc–Zr alloys. Mater Sci Eng A. 2019;739:427.
[52] Wen SP, Gao KY, Huang H, Wang W, Nie ZR. Precipitation evolution in Al–Er–Zr alloys during aging at elevated temperature. J Alloys Compd. 2013;574:92.
[53] Wen SP, Gao KY, Li Y, Huang H, Nie ZR. Synergetic effect of Er and Zr on the precipitation hardening of Al–Er–Zr alloy. Scr Mater. 2011;65(3):592.
[54] Wu H, Wen SP, Wu XL, Gao KY, Huang H, Wang W, Nie ZR. A study of precipitation strengthening and recrystallization behavior in dilute Al–Er–Hf–Zr alloys. Mater Sci Eng A. 2015;639:307.
[55] Wen SP, Xing ZB, Huang H, Li BL, Wang Z, Nie ZR. The effect of erbium on the microstructure and mechanical properties of Al–Mg–Mn–Zr alloy. Mater Sci Eng A. 2009;516:42.
[56] Zhang YZ, Gu J, Tian Y, Gao HY, Wang J, Sun BD. Microstructural evolution and mechanical property of Al–Zr and Al–Zr–Y alloys. Mater Sci Eng A. 2014;616:132.
[57] Marquis EA, Seidman DN, Asta M, Woodward C. Composition evolution of nanoscale Al_3Sc precipitates in an Al–Mg–Sc alloy: experiments and computations. Acta Mater. 2006;54(1):119.
[58] Marquis EA, Seidman DN, Asta M, Woodward C, Ozoliņš V. Mg segregation at Al/Al_3Sc heterophase interfaces on an atomic scale: experiments and computations. Phys Rev Lett. 2003;91(23):036101.
[59] Feng L, Li JG, Mao YZ. Strengthening and toughening mechanism of high-Mg low-Sc Al–Mg–Sc–Zr alloy. Rare Met Mater Eng. 2019;48(9):2857.
[60] Tang L, Peng XY, Huang JW, Ma AB, Deng Y, Xu GF. Microstructure and mechanical properties of severely deformed Al–Mg–Sc–Zr alloy and their evolution during annealing. Mater Sci Eng A. 2019;754:295.
[61] Li RD, Chen H, Chen C, Zhu HB, Wang MB, Yuan TC, Song B. Selective laser melting of gas atomized Al–3.02Mg–0.2Sc–0.1Zr alloy powder: microstructure and mechanical properties. Adv Eng Mater. 2019;21(3):1800650.
[62] Luo XE, Fang HJ, Liu H, Yan Y, Zhu HL, Yu K. Effect of Sc and Zr on Al–6(Mn, Fe) Phase in Al–Mg–Mn Alloys. Mater Trans. 2019;60(5):737.
[63] Chanyathunyaroj K, Patakham U, Kou S, Limmaneevichitr C. Mechanical properties of squeeze-cast Al–7Si–0.3Mg alloys with Sc-modified Fe-rich intermetallic compounds. Rare Met. 2018;37(9):769.
[64] Lu Z, Zhang LJ, Wang J, Yao QL, Rao GH, Zhou HY. Understanding of strengthening and toughening mechanisms for Sc-modified Al–Si–(Mg) series casting alloys designed by computational thermodynamics. J Alloys Compd. 2019;805:415.
[65] Kobayashi KF, Hogan LM. The crystal growth of silicon in Al–Si alloys. J Mater Sci. 1985;20(4):1961.
[66] Mao GL, Yan H, Zhu CC, Wu Z, Gao WL. The varied mechanisms of yttrium (Y) modifying a hypoeutectic Al–Si alloy under conditions of different cooling rates. J Alloys Compd. 2019;806:909.
[67] Yu SS, Wang RC, Peng CQ, Cai ZY, Wu X, Feng Y, Wang XF. Effect of minor scandium addition on the microstructure and properties of Al–50Si alloys for electronic packaging. J Mater Sci Mater Electron. 2019;30:20770–7.
[68] Chen Y, Liu CY, Ma ZY, Huang HF, Peng YH, Hou YF. Effect of Sc addition on the microstructure, mechanical properties, and damping capacity of Al–20Zn alloy. Mater Charact. 2019;157:109892.
[69] Jia QB, Rometsch P, Kurnsteiner P, Chao Q, Huang AJ, Weyland M, Bourgeois L, Wu XH. Selective laser melting of a high strength Al–Mn–Sc alloy: alloy design and strengthening mechanisms. Acta Mater. 2019;171:108.
[70] Suwanpreecha C, Pandee P, Patakham U, Limmaneevichitr C. New generation of eutectic Al–Ni casting alloys for elevated temperature services. Mater Sci Eng A. 2018;709:46.
[71] Belov NA, Alabin AN, Eskin DG. Improving the properties of cold-rolled Al–6%Ni sheets by alloying and heat treatment. Scr Mater. 2004;50(1):89.

[72] Nakagawa YG, Weatherly GC. The thermal stability of the rod Al_3Ni–Al eutectic. Acta Metall. 1972;20(3):345.
[73] Fan Y, Makhlouf M. The Al–Al_3Ni eutectic reaction: crystallography and mechanism of formation. Metall Mater Trans. 2015;46(9):3808.
[74] Suwanpreecha C, Toinin JP, Michi RA, Pandee P, Dunand DC, Limmaneevichitr C. Strengthening mechanisms in Al–Ni–Sc alloys containing Al_3Ni microfibers and Al_3Sc nanoprecipitates. Acta Mater. 2019;164:334.
[75] Chen BA, Pan L, Wang RH, Liu G, Cheng PM, Xiao L, Sun J. Effect of solution treatment on precipitation behaviors and age hardening response of Al–Cu alloys with Sc addition. Mater Sci Eng A. 2011;530:607.
[76] Jiang L, Li JK, Liu G, Wang RH, Chen BA, Zhang JY, Sun J, Yang MX, Yang G, Yang J, Cao XZ. Length-scale dependent microalloying effects on precipitation behaviors and mechanical properties of Al–Cu alloys with minor Sc addition. Mater Sci Eng A. 2015;637:139.
[77] Gao YH, Kuang J, Liu G, Sun J. Effect of minor Sc and Fe co-addition on the microstructure and mechanical properties of Al–Cu alloys during homogenization treatment. Mater Sci Eng A. 2019;746:11.
[78] Gao YH, Yang C, Zhang JY, Cao LF, Liu G, Sun J, Ma E. Stabilizing nanoprecipitates in Al–Cu alloys for creep resistance at 300 °C. Mater Res Lett. 2019;7(1):18.
[79] Zhao MQ, Xing Y, Jia ZH, Liu Q, Wu XZ. Effects of heating rate on the hardness and microstructure of Al–Cu and Al–Cu–Zr–Ti–V alloys. J Alloys Compd. 2016;686:312.
[80] Hu H, Zhao MQ, Wu XZ, Jia ZH, Wang R, Li WG, Liu Q. The structural stability, mechanical properties and stacking fault energy of Al_3Zr precipitates in Al–Cu–Zr alloys: HRTEM observations and first-principles calculations. J Alloys Compd. 2016;681:96.
[81] Biswas A, Siegel DJ, Seidman DN. Simultaneous segregation at coherent and semicoherent heterophase interfaces. Phys Rev Lett. 2010;105(7):076102.
[82] Chen BA, Liu G, Wang RH, Zhang JY, Jiang L, Song JJ, Sun J. Effect of interfacial solute segregation on ductile fracture of Al–Cu–Sc alloys. Acta Mater. 2013;61(3):1676.
[83] Yang C, Zhang P, Shao D, Wang RH, Cao LF, Zhang JY, Liu G, Chen BA, Sun J. The influence of Sc solute partitioning on the microalloying effect and mechanical properties of Al–Cu alloys with minor Sc addition. Acta Mater. 2016;119:68.
[84] Shin DW, Shyam A, Lee SK, Yamamoto Y, Haynes JA. Solute segregation at the Al/θ′–Al_2Cu interface in Al–Cu alloys. Acta Mater. 2017;141:327.
[85] Dorin T, Ramajayam M, Lamb J, Langan T. Effect of Sc and Zr additions on the microstructure/strength of Al–Cu binary alloys. Mater Sci Eng A. 2017;707:58.
[86] Yao DM, Zhao WG, Zhao HL, Qiu F, Jiang QC. High creep resistance behavior of the casting Al–Cu alloy modified by La. Scr Mater. 2009;61(3):1153.
[87] Wang WT, Zhang XM, Gao ZG, Jia YZ, Ye LY, Zheng DW, Liu L. Influences of Ce addition on the microstructures and mechanical properties of 2519A aluminum alloy plate. J Alloys Compd. 2010;491:366.
[88] Xiao DH, Wang JN, Ding DY, Yang HL. Effect of rare earth Ce addition on the microstructure and mechanical properties of an Al–Cu–Mg–Ag alloy. J Alloys Compd. 2003;352:84.
[89] Bai S, Yi XL, Liu GH, Liu ZY, Wang J, Zhao JG. Effect of Sc addition on the microstructures and age-hardening behavior of an Al–Cu–Mg–Ag alloy. Mater Sci Eng. 2019;756:258.
[90] Gupta AK, Lloyd DJ, Court SA. Precipitation hardening in Al–Mg–Si alloys with and without excess Si. Mater Sci Eng A. 2001;316:11.
[91] Zhong H, Rometsch PA, Estrin Y. The influence of Si and Mg content on the microstructure, tensile ductility, and stretch formability of 6xxx alloys. Metall Mater Trans A. 2013;44(13):3970.
[92] Jiang SY, Wang RH. Grain size-dependent Mg/Si ratio effect on the microstructure and mechanical/electrical properties of Al–Mg–Si–Sc alloys. J Mater Sci Technol. 2019;35(7):1354.
[93] Dorin T, Ramajayam M, Babaniaris S, Jiang L, Langan TJ. Precipitation sequence in Al–Mg–Si–Sc–Zr alloys during isochronal aging. Materialia. 2019;8(1):100437.
[94] Liu YH, Yan LM, Hou XH, Huang DN, Zhang JB, Shen J. Precipitates and corrosion resistance of an Al–Zn–Mg–Cu–Zr plate with different percentage reduction per passes. Rare Met. 2018;37(5):381.
[95] Deng Y, Yin ZM, Zhao K, Duan JQ, Hu J, He ZB. Effects of Sc and Zr microalloying additions and aging time at 120 °C on the corrosion behaviour of an Al–Zn–Mg alloy. Corros Sci. 2012;65(1):288.
[96] Shi YJ, Pan QL, Li MJ, Huang X, Li B. Effect of Sc and Zr additions on corrosion behaviour of Al–Zn–Mg–Cu alloys. J Alloys Compd. 2014;612:42.
[97] Wang Y, Xiong BQ, Li ZH, Huang SH, Wen K, Li XW, Zhang YA. As-cast microstructure of Al–Zn–Mg–Cu–Zr alloy containing trace amount of Sc. Rare Met. 2019;38(4):343.
[98] Deng Y, Yin ZM, Zhao K, Duan JQ, He ZB. Effects of Sc and Zr microalloying additions on the microstructure and mechanical properties of new Al–Zn–Mg alloys. J Alloys Compd. 2012;530:71.
[99] Li G, Zhao NQ, Liu T, Li JJ, He CN, Shi CS, Liu EZ, Sha JW. Effect of Sc/Zr ratio on the microstructure and mechanical properties of new type of Al–Zn–Mg–Sc–Zr alloys. Mater Sci Eng A. 2014;617:219.
[100] Liu L, Cui XY, Jiang JT, Zhang B, Nomoto K, Zhen L, Ringer SP. Segregation of the major alloying elements to Al–3(Sc, Zr) precipitates in an Al–Zn–Mg–Cu–Sc–Zr alloy. Mater Charact. 2019;157:109898.
[101] Zhang F, Su XK, Chen ZY, Nie ZR. Effect of welding parameters on microstructure and mechanical properties of friction stir welded joints of a super high strength Al–Zn–Mg–Cu aluminum alloy. Mater Des. 2015;67(2):483.
[102] Wu H, Wen SP, Huang H, Gao KY, Wu XL, Wang W, Nie ZR. Hot deformation behavior and processing map of a new type Al–Zn–Mg–Er–Zr alloy. J Alloys Compd. 2015;685:869.

Dr. Gang Liu is currently a professor in the School of Materials Science and Engineering at Xi'an Jiaotong University. He received his Ph.D. degree in Materials Science and Engineering from Xi'an Jiaotong University in 2002. He worked as a postdoctor in Tsinghua University during 2003–2005 and as an Alexander von Humboldt Research Fellow in Leibniz Institute for Solid State Materials Research at Dresden, Germany, from 2008 to 2009. He has published 180 peer-reviewed papers. His research interests focus on the alloy design and microstructural controlling of advanced metal alloys with enhanced performance.